Energy Conversion and Management 50 (2009) 1236–1243

Contents lists available at ScienceDirect

Energy Conversion and Management

journal homepage: www.elsevier.com/locate/enconman

Study of thermoelectric systems applied to electric power generation

A. Rodríguez, J.G. Vián *, D. Astrain, A. Martínez

Dpto. Ingeniería Mecánica, Energética y de Materiales, Universidad Pública de Navarra, Pamplona, Spain

ARTICLE INFO

Article history:
Received 3 July 2007
Received in revised form 27 June 2008
Accepted 27 January 2009
Available online 28 February 2009

Keywords:
Thermoelectric
Power generation
Heat transfer
Computational model
Residual heat

ABSTRACT

A computational model has been developed in order to simulate the thermal and electric behavior of thermoelectric generators. This model solves the nonlinear system of equations of the thermoelectric and heat transfer equations. The *inputs* of the program are the thermoelectric parameters as a function of temperature and the boundary conditions, (room temperature and residual heat flux). The *outputs* are the temperature values of all the elements forming the thermoelectric generator, (performance, electric power, voltage and electric current generated). The model solves the equation system using the finite difference method and semi-empirical expressions for the convection coefficients.

A thermoelectric electric power generation test bench has been built in order to validate and determine the accuracy of the computational model, which maximum error is lower than 5%.

The objective of this study is to create a design tool that allows us to solve the system of equations involved in the electric generation process without needing to impose boundary conditions that are not known in the design phase, such as the temperature of the Peltier modules.

With the computational model, we study the influence of the heat flux supplied as well as the room temperature on the electric power generated.

1. Introduction

We have developed a computational model that simulates the thermal and electric behavior of a thermoelectric generator that presents some advantages with respect to previous ones.

Some applications in thermoelectric generation use waste heat fluxes as energy source. Benson et al. [1] investigated geothermal heat fluxes with temperature gaps of 80–180 °C; other gaps are produced in the ocean's currents, in solar panels, or in power generator stations. Matsuura and Rowe [2] propose these and other residual thermal energy sources.

In order to study these applications, it is necessary to determine the behavior of the thermoelectric devices. The analytic solution most used to solve the equation system of the thermoelectric device is the ideal thermoelectric couple, which expression was obtained by Ioffe in [3]. Other references that use this expression are [4,5], and in the case of thermoelectric generation, it was used in [6–11]. In the expression of the ideal thermoelectric couple, the thermoelectric parameters (Seebeck coefficient, electrical resistivity and thermal conductivity) are not dependent on the temperature.

A better approximation is to consider an average value of the Seebeck coefficient within the operating temperatures of the thermoelectric couple, as can be seen in the researches of Ioffe in [3], Arenas, in [12] and Yu in [13]. Nevertheless, this approximation does not adjust to reality because, in fact, the Seebeck coefficient varies with temperature.

The Buist works [14,15] divide a thermoelement into segments and apply the ideal thermoelectric couple in each segment. This model keeps in mind the variation of the thermoelectric properties with temperature. Its major disadvantage is that the model needs the heat flux, the hot source temperature and the electric current generated as input parameters, and it is necessary to obtain them experimentally.

To determine completely the thermoelectric device behavior, it is also necessary to consider the heat exchangers on the sides of the Peltier module, as is described by Stockholm in [16]. The disadvantage of Stockholm's model is that it simplifies the Peltier module, and it is impossible to optimize the geometry and dimensions. Similar, but more comprehensive, models have been posed by Arenas in [12] and by Kondraitev in [17], but these models do not calculate the transitory state.

Our model is based on a computational model developed to simulate the behavior of thermoelectric refrigerators by Vián and Astrain [18–20].

Our model solves the behavior of the thermoelectric generator and makes improvements to the previous models. It takes into account the properties of the thermoelectric materials as functions of temperature. We divide the Peltier module into ten different parts, which allows us to determine the variation of the thermoelectric properties in its interior. The Thomson effect is not considered

* Corresponding author. Tel.: +34 948169309; fax: +34 948169099.
E-mail address: vian@unavarra.es (J.G. Vián).

0196-8904/$ - see front matter © 2009 Elsevier Ltd. All rights reserved.
doi:10.1016/j.enconman.2009.01.036

Nomenclature

A	area (m^2)
C	thermal capacity ($J\,K^{-1}$)
c	specific heat ($J\,kg^{-1}\,K^{-1}$)
E_t	electromotive force (V)
I	electric current (A)
k	thermal conductivity ($W\,m^{-1}\,K^{-1}$)
L	characteristic length (m)
m	load ratio (R_L/R_O)
N	number of thermocouples of Peltier modules
P	generated power (W)
$\dot{Q}$	calorific power (W)
$\overset{*}{q}$	calorific power per unit volume ($W\,m^{-3}$)
R	thermal resistance ($K\,W^{-1}$)
R_{cont}	contact electric resistance (Ω)
R_O	electric resistance of Peltier module (Ω)
R_L	load electric resistance (Ω)
T	temperature (°C)
T	temperature (K)
T'	temperature in next time step (K)
V	volume (m^3)

Greek letters

α	seebeck coefficient (V/K)
ΔV	difference of electric power (V)
ΔT	difference of temperatures (K)
ε	test
ρ	density ($kg\,m^{-3}$)
ρ_0	electric resistance of Peltier module ($\Omega\,m$)
σ	thomson coefficient ($V\,K^{-1}$)
τ	time (s)

Superscripts, subscripts

c	cold side of Peltier module
cont	semiconductor and copper contact
Dissip	dissipater
h	hot side of Peltier module
i	node i
in	system inlet
k	number of ε repetitions
J	joule effect
j	node j
leaks	system loses
max	maximum value of studied curve
out	system outlet
er	electric resistance of generation of heat flux
relat	relative
room	ambient

negligible, which gives an approximation closer to reality. The model *inputs* are only the room temperature and the heat flux supplied by the residual energy source; it is not necessary to obtain the parameters experimentally.

The heat exchangers of the hot and cold side are included in our model; and therefore, the temperatures and heat fluxes in all the components of the thermoelectric system can be obtained as *outputs*. Another advantage is that our model determines the transitory state as well as the steady state.

2. Objectives

The objectives we have proposed are:

- A computational model design capable to simulate the thermoelectric generator operation, including the heat transfer from the thermal sources to the faces of the Peltier module. We will keep in mind the Thompson coefficient and all the thermoelectric properties will be a function of the temperature.
- Validation of the computational model with experimental data obtained from the test bench.
- Theoretical and experimental study of the influence on the thermoelectric power generated of the following parameters:
  - Residual heat flux and electric load resistance for a constant room temperature.
  - Room temperature and electric load resistance for a constant residual heat flux.
  - Room temperature and electric load resistance for a constant temperature gap between the faces of the Peltier module.

3. Computational model

In thermoelectric devices, for both refrigeration and generation applications, the temperatures of the faces of the Peltier modules and in the internal nodes can not be determined analytically without knowing the heat flux due to the thermoelectric effects. The system of equations in order to calculate the temperatures is nonlinear.

The model solves these nonlinear systems, formed by the thermoelectricity equations and the heat transfer equations, by the finite difference method, which calculates the temperature at different points separated in space by a discrete distance. In the transient state, the temperatures of these points are calculated at discrete periods of time. With this purpose, a finite period of time is chosen and the temperatures for all the points are recalculated at the end of this time interval.

While solving the model using the implicit finite difference method, the values of heat flux can be determined using the values of the temperatures of the time step before.

The *inputs* of the model are: the geometric data and the material properties of the elements of the thermoelectric system studied (thermal conductivity, electric resistivity, Seebeck coefficient and specific heat), and the thermal energy value supplied to the system. After the simulation, the *outputs* of the model are: the values of efficiency, electric voltage and current, electric power generated, temperatures and heat flux generated.

Previous works, showed in Refs. [3–13], needed the temperature values on the Peltier module faces as *inputs* for their models. These were experimentally measured in the thermoelectric generation system for each heat flux supplied.

Our model can determine all the heat fluxes and temperatures of the thermoelectric generator components with only the heat flux supplied by the residual energy source and the room temperature as *inputs*. This model does not need previous experimental values of the device temperatures.

3.1. Hypothesis of the model

The materials used in the test bench shown in Fig. 2 are considered isotropic.

The model has been built neglecting the magnetic field effects, so the Hall, Nernst, Ettingshausen and Righi-Ludec effects are neglected as well.

3.2. Equations of the model

The model solves the equation of heat transfer in transitory state for one dimension and one dimensional flow:

$$\rho c_p \delta T/\delta\tau = k(\delta^2 T/\delta x^2) + q^* \tag{1}$$

The equation of heat conduction (1) multiplied by the volume and applied to the ith node as a function of the thermal resistances and capacities is:

$$(T'_{i-1} - T'_i)/R_{i-1,i} + (T'_j - T'_i)/R_{i,j} + \dot{Q}_i = (T'_i - T_i)C_i/\delta\tau \tag{2}$$

The generation or absorption of heat related to node i is represented by $\dot{Q}_i$, and its expression is given by Eqs. (6)–(9).

The thermal resistance between nodes i and j, Eq. (3), and the thermal capacity of node i, Eq. (4), are:

$$R_{i,j} = L_{ij}/(k_i A_i) \tag{3}$$

$$C_i = V_i \rho_i c_p \tag{4}$$

Therefore, the thermal resistance and capacity of the Peltier module is studied as in [18]; in our case, we divide the module into ten nodes, and we get a thermal resistance between nodes and a thermal capacity associated with each node as a function of its temperature.

$$\dot{Q}_h = -N2\alpha_h I T_h + I^2 R_{cont} \tag{6}$$

$$\dot{Q}_c = N2\alpha_c I T_c + I^2 R_{cont} \tag{7}$$

$$\dot{Q}_J = I^2 R_0 = N I^2 2\rho L/A \tag{8}$$

$$\dot{Q}_\sigma = \sigma I \Delta T \tag{9}$$

The temperature of the semiconductor terminals is used to calculate the heat fluxes due to the Peltier effect. The contribution of the contact thermal effects was developed in [2].

The discretization of the thermoelectric generator uses symbols of an electric analogy, shown in Fig. 1. The model assigns different nodes to the Peltier module in the ceramic part and in the end of the semiconductor, and thus, it is not necessary to correct the temperature gap between them. This is an improvement to the analytic solution of [2], which is necessary when only the experimental temperature of the ceramic part of the Peltier module is available.With the scheme shown in Fig. 1 and Eq. (5), we obtain the following system of equations:

$$[M]\left[T'_i\right] = [T_i] + \partial\tau/C_i\left[\dot{Q}_i\right] \tag{10}$$

The matrix system (10) is developed as a function of the thermal resistances and capacities of the device, as shown in Eq. (11):

$$\begin{bmatrix}
1+\frac{\delta\tau}{C_1R_{1-2}} & -\frac{\delta\tau}{C_1R_{1-2}} & 0 & 0 & -\frac{\delta\tau}{C_1R_{1-5}} & 0 & & 0 & -\frac{\delta\tau}{C_1R_{1-16}} & 0 \\
-\frac{\delta\tau}{C_2R_{1-2}} & 1+\frac{\delta\tau}{C_2}\left(\frac{1}{R_{1-2}+R_{2-3}}\right) & -\frac{\delta\tau}{C_2R_{2-3}} & 0 & & & & & & 0 \\
0 & -\frac{\delta\tau}{C_3R_{2-3}} & 1+\frac{\delta\tau}{C_3}\left(\frac{1}{R_{2-3}+R_{3-4}}\right) & -\frac{\delta\tau}{C_3R_{3-4}} & & & & & & \\
0 & 0 & -\frac{\delta\tau}{C_4R_{3-4}} & * & * & & & & & \\
-\frac{\delta\tau}{C_5R_{1-5}} & & & * & * & * & & & & -\frac{\delta\tau}{C_5R_{5-17}} \\
0 & & & & * & * & * & & & \\
 & & & & * & * & * & 0 & 0 & \\
0 & & & & & -\frac{\delta\tau}{C_{15}R_{14-15}} & 1+\frac{\delta\tau}{C_{15}\left(R_{14-15}+R_{15-16}+R_{15-17}\right)} & -\frac{\delta\tau}{C_{15}R_{15-16}} & -\frac{\delta\tau}{C_{15}R_{15-17}} & \\
-\frac{\delta\tau}{C_{16}R_{1-16}} & & & & & 0 & -\frac{\delta\tau}{C_{16}R_{15-16}} & 1+\frac{\delta\tau}{C_{16}}\left(\frac{1}{R_{1-16}+R_{15-16}}\right) & 0 & \\
0 & 0 & & & -\frac{\delta\tau}{C_{17}R_{5-17}} & 0 & -\frac{\delta\tau}{C_{17}R_{15-17}} & 0 & 1+\frac{\delta\tau}{C_{17}}\left(\frac{1}{R_{16-17}+R_{5-17}}\right)
\end{bmatrix} \times \begin{bmatrix} T_1^i \\ T_2^i \\ * \\ * \\ * \\ * \\ * \\ * \\ T_{17}^i \end{bmatrix} = \begin{bmatrix} T_1^i \\ T_2^i \\ * \\ * \\ * \\ * \\ * \\ * \\ T_{17}^i \end{bmatrix} + \begin{bmatrix} 0 \\ \frac{\dot{Q}_2\delta\tau}{C_2} \\ 0 \\ 0 \\ 0 \\ \frac{\dot{Q}_6\delta\tau}{C_6} \\ * \\ \frac{\dot{Q}_{14}\delta\tau}{C_{14}} \\ 0 \\ 0 \\ 0 \end{bmatrix} \tag{11}$$

For the contact resistances between the elements of the test bench, the works of Ritzer and Lau [21] were used.

The thermal resistance and capacity of the heat extender are calculated using Eqs. (3) and (4), giving the following values:

$$R_{Heat\ Extender} = 0.1677\,[\mathrm{K/W}]$$

$$C_{Heat\ Extender} = 211\,[\mathrm{J/kg\,K}]$$

In our case, the thermal resistance of the dissipater and the insulator related to the ambient are calculated experimentally as described below:

Grouping the equation parameters as functions of the node temperatures and the heat flux, we obtain the equation:

$$-T'_{i-1}\delta\tau/(C_iR_{i-1,i}) + T'_i[\delta\tau/C_i(1/R_{i-1,i} + 1/R_{i,j}) + 1] - T'_j\delta\tau/C_iR_{i,j} = T_i + \dot{Q}_i\delta\tau/C_i \tag{5}$$

The model incorporates the equations from the thermoelectric effects. These effects are the heat flux from the Peltier effects, Eqs. (6) and (7), Joule Eq. (8) and Thomson Eq. (9), with no magnetic fields.

The Seebeck coefficient is a parameter variable with the temperatures, so if it is included in the model as a function of the temperature, we get the following expressions for the electromotive force generated due to the Seebeck effect, the voltage in the ends of the generator, the current and the electric power.

$$E_t = 2N\left((\alpha_h T_h - \alpha_c T_c) - \sum_{i=1}^{10}\sigma_i(T_i - T_{i+1})\right) \tag{12}$$

$$\Delta V = (m/1+m)E_t \tag{13}$$

$$I = E_t/(1+m)R_0 \tag{14}$$

$$P_{out} = \Delta V I \tag{15}$$

4. Experimental work

The assembly of the test bench, Fig. 2, has been designed for this work, and it is composed of:

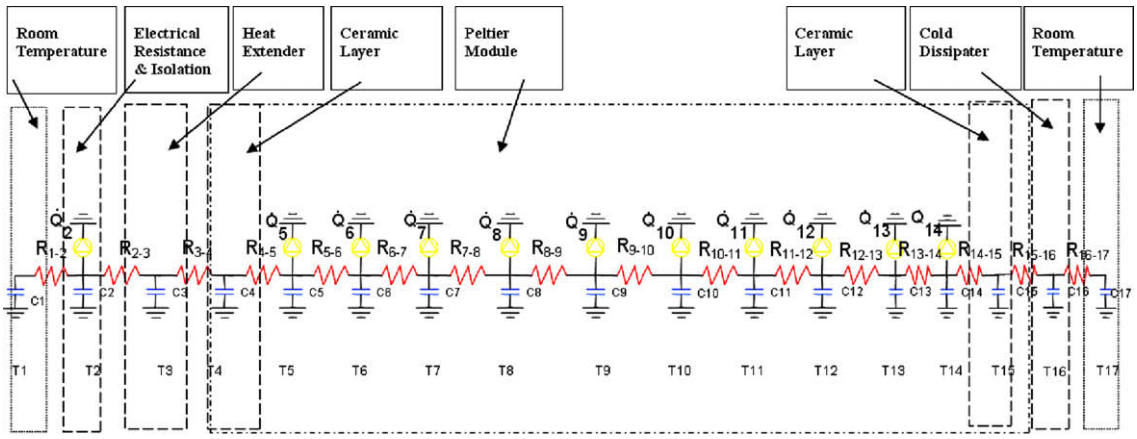

Fig. 1. Scheme of the thermal-electric analogy of the computational model.

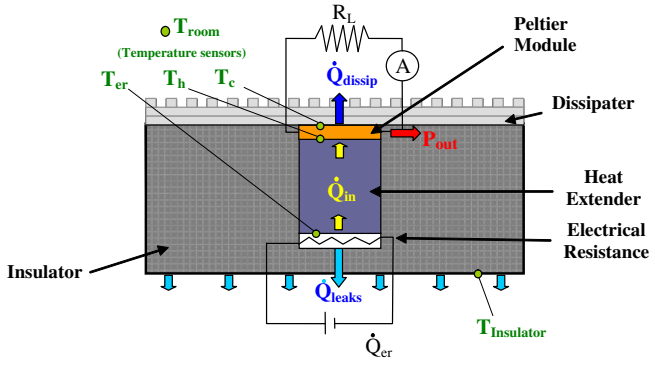

Fig. 2. Scheme of the test bench.

- A calibrated electric resistance that simulates the thermal energy source, providing a heat flux $\dot{Q}_{er}$ with a maximum value of 50 W.
- A heat extender, with a known thermal resistance that communicates the electric resistance with the Peltier module.
- A Peltier module Marlow DT12-6L type.
- A dissipater for the cold side of the Peltier module, with a thermal resistance experimentally determined.
- A decade box, CAM METRIC R420, in order to be able to simulate with different load resistances.

The principal element of study is the Peltier module, Marlow DT12-6L, used generally in thermoelectric refrigeration. We have chosen this module to take advantage of residual thermal energies of low temperature, (lower than 85 °C), as its temperature range is the most suitable.

In order to determinate with accuracy the thermal resistance of the dissipater, we made some tests in a standardized climatic room. The tests were made with a prototype that used a known heat flux that went through the dissipater with the same temperature room conditions as those of the thermoelectric generator.

In Fig. 2, it can be seen that the heat flux that goes through the heat extender is the same as the heat absorbed by the Peltier module $\dot{Q}_{in}$. This is calculated with the temperature gap between the ends of the heat extender and the thermal resistance of the heat extender using Eq. (16).

$$\dot{Q}_{in} = \Delta T_{Heat\ Extender} / R_{Heat\ Extender} \tag{16}$$

In an open circuit case ($R_L = 0$), there is no Peltier effect, and thus, there is no electric power generated in the Peltier module ($P_{out} = 0$), so the heat flux absorbed is $\dot{Q}_{in}$, and fits with the flux through the dissipater $\dot{Q}_{Dissip}$; With this data and experimentally measuring the temperature gap between the dissipater and the ambient, we determined the thermal resistance of the dissipater using Eq. (17).

$$R_{Dissip} = \Delta T_{Dissip-Ambient} / Q_{Dissip} \tag{17}$$

Table 1
Thermal resistance of the dissipater.

$\dot{Q}_{Dissip.}$ [W]	$\Delta T_{Dissip\text{-}Ambient}$ (K)	R_{Dissip} (k/W)
25.93	21.8	0.84
21.54	18.1	0.84
18.35	15.2	0.83
13.96	11.4	0.82
9.17	7.6	0.83
4.39	3.7	0.84

In Table 1, the values of the thermal resistance for different heat fluxes of the dissipater $\dot{Q}_{Dissip}$ are shown. The data of the thermal resistance of the dissipater are independent of the thermoelectric device installed, and the thermal resistance of the dissipater is an input data for the model.

The temperature probes are thermocouples of K type, and the data logging is ALMEMO 5590-2. A thermocouple is placed in each point of study shown in Fig. 2. The tests were placed in a climatic room, CLIMATS 1440H 60/3, to keep the room temperature constant.

The heat flux due to the leaks, Eq. (19), is the difference between the heat fluxes generated by the electric resistance, Eq. (18), and that absorbed by the Peltier module, Eq. (16).

$$\dot{Q}_{er} = \Delta V_{er} I_{er} \tag{18}$$

$$\dot{Q}_{leaks} = \dot{Q}_{er} - \dot{Q}_{in} \tag{19}$$

The thermal resistance between the electric resistance and the ambient is determined using the same methodology that was used to calculate the thermal resistance of the dissipater, using two thermocouples, one placed in the ambient and the other in the electric resistance. Then the temperature gap between the electric resistance and the ambient is known. Thus, with the value of the heat flux that is transmitted, we calculate the thermal resistance as is shown in Table 2 for different values of the incoming flux.

In order to study the electric power generated, it is necessary to keep in mind the load resistance of the device joint to the thermoelectric generator. To simulate this load resistance a decade box has been used, CAM METRIC R420, which provides a variable resistance from 0.01 Ω to 100 Ω.

Table 2
Thermal resistance between the thermal generator source and the room.

$\dot{Q}_{er}$ [(W)]	$\dot{Q}_{in}$ [(W)]	$\dot{Q}_{leaks}$ [(W)]	$\Delta T_{\text{Electr.Resist-Ambient}}$ (K)	$R_{\text{Electr.Resist-Ambient}}$ (K/W)
29.7	25.9	3.8	76.2	20.1
24.5	21.5	2.9	65.7	22.4
21.0	18.4	2.7	56.7	21.4
15.4	14.0	1.4	34.6	24.7
10.3	9.2	1.1	25.7	23.4
5.1	4.4	0.7	13.8	20.0

5. Results and discussion

The experimental data obtained from the test bench are compared with the values from the computational model. With this comparison, we make a validation of the model to determine the error between the experimental and the simulated values.

The sample mean $\overline{P}_{out,\varepsilon}$ of the measurement results is estimated from 10 independent observations of P_{ε} obtained under the same conditions of measurement.

$$\overline{P}_{out,\varepsilon} = \frac{1}{n}\sum_{k=1}^{10} P_{out,\varepsilon,k} \tag{20}$$

The standard uncertainty $u(P_{out,\varepsilon})$ associated with $\overline{P}_{out,\varepsilon}$ is the estimated standard deviation of the mean, given by the expression.

$$u(P_{out,\varepsilon}) = \left(\frac{1}{n(n-1)}\sum_{k=1}^{10}(P_{out,\varepsilon,k} - \overline{P}_{out,\varepsilon})^2\right)^{1/2} \tag{21}$$

Therefore, the relative uncertainty of the experimental measurement is estimated as follows:

$$u_{relat}(P_{out,\varepsilon}) = \frac{u(P_{out,\varepsilon})}{\overline{P}_{out,\varepsilon}} \tag{22}$$

The total relative uncertainty of the experiments was acceptable. It was lower than 1.5% in the case of output power and lower than 2% in the case of temperatures.

In order to study the output power of the thermoelectric generator system, we have analyzed three different cases:

(I) Constant room temperature, varying the residual heat flux and the load electric resistance.
(II) Constant residual heat flux, varying the room temperature and the load electric resistance.
(III) Constant temperature gap between the Peltier module, varying the room temperature and the load electric resistance.

The model we present in this work can determine the temperatures and the heat fluxes of all nodes of the thermoelectric generation system components. It only needs as input the heat flux supplied from the hot source and the room temperature. It is not necessary to know previously the electric current as in [16], or [17]. In our case, the current is not an input parameter but an output parameter related with all the unknowns by Eq. (14); moreover, it uses the thermoelectric parameters as a function of temperature.

5.1. Case I: Constant room temperature varying the residual heat flux and the load electric resistance

5.1.1. Computational model validation

In the tests developed for the present case, the heat flux was constant. This heat flux simulates the residual thermal energy. The electric power obtained is measured for each of the load resistances tested.

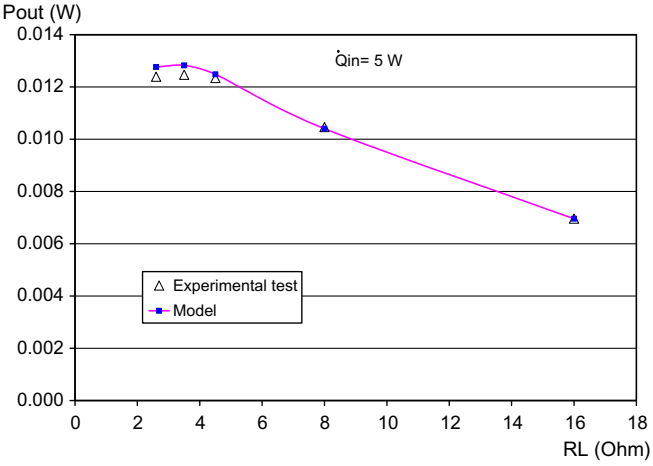

Fig. 3. Comparison of the power generated from the model and the experimental data for a heat flux of 5 W.

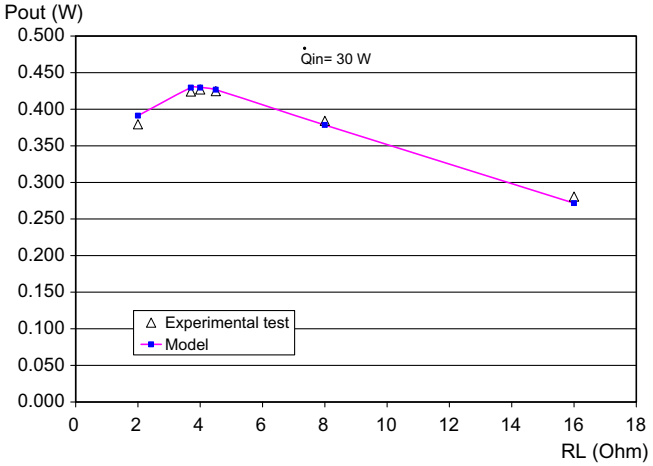

Fig. 4. Comparison of the electric power generated by the model and experimental data for a supplied heat flux of 30 W.

Figs. 3 and 4 show a comparison of the model and the experimental values for residual heat fluxes of $\dot{Q}_{in} = 5\,W$ and $\dot{Q}_{in} = 30\,W$, respectively. The values are acceptable, with an error lower than 5%.

The maximum electric power is produced for values of load resistance equal to the internal resistance of the Peltier module. This behavior was demonstrated analytically in [2]. For a constant room temperature, the greater is the supplied residual heat flux, the higher is the temperature of the Peltier module.

5.1.2. Output thermoelectric power – experimental and simulated

Our model has into account the variation of the electric resistance of the Peltier module with temperature. Thus, the load

electric resistance that gives the maximum power increases, with the temperature, as the internal electric resistance of the Peltier module increases with the temperature as well. As an example, it can be seen that if a heat flux of 30 W is supplied, the load resistance value for the maximum power generated is 3.9 Ω, and if the heat flux has a value of 5 W, the load resistance increases only to 3.3 Ω, which makes the rise 18%. This effect is shown in Fig. 5.

With the analytical solution of the ideal thermoelectric couple developed from Refs. [3–11] or in the models that use average values of the thermoelectric parameters, Refs. [12,13], the power and efficiency curves are calculated as a function of the electric current generated, keeping constant the temperature gap between the faces of the Peltier module.

With the models of the mentioned works it is not possible to determine the effect shown in Fig. 5. As a matter of fact, increasing the supplied heat flux causes the absorbed heat due to the Peltier effect to increase. Thus, the temperature gap between the Peltier module's faces increases. In the cases of the works from Refs. [3–11], it would be necessary to calculate experimentally the temperature of the faces of the Peltier module each time the heat flux varies in order to determine the generated thermoelectric power.

5.1.3. Temperature gap between the sides of the Peltier module – experimental and simulated

The model calculates the temperatures and the heat fluxes of all the elements of the thermoelectric device. As can be seen in Fig. 6, for a constant heat flux supplied, when the load resistance R_L increases, the temperature gap between the faces of the Peltier module increases (ΔT) too. The simulation results with the model have very good accuracy, with errors lower than 5% with the experimental results. As an example, let us see what happens for a supplied heat flux of 30 W where the temperature gap between the faces of the Peltier module increases 10 K (which makes an increase of 27%) when the load resistance is varied from 2 Ω to 16 Ω.

5.2. Case II: Constant waste heat flux varying the room temperature and the electric load resistance

5.2.1. Output thermoelectric power experimental and simulated

For the tests made for a constant heat flux of 9.97 W and varying the room temperature from −25 °C to 50 °C, Fig. 7 shows that the experimental values obtained of generated power vary with the room temperature. This fact is due to the variation of the thermoelectric properties as a function of temperature.

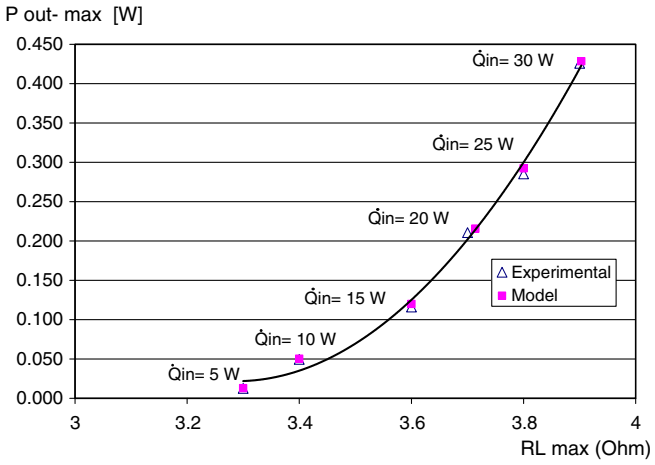

Fig. 5. Thermoelectric generated power maximum for each curve of heat flux constant with a room temperature of T_{room} = 273 K.

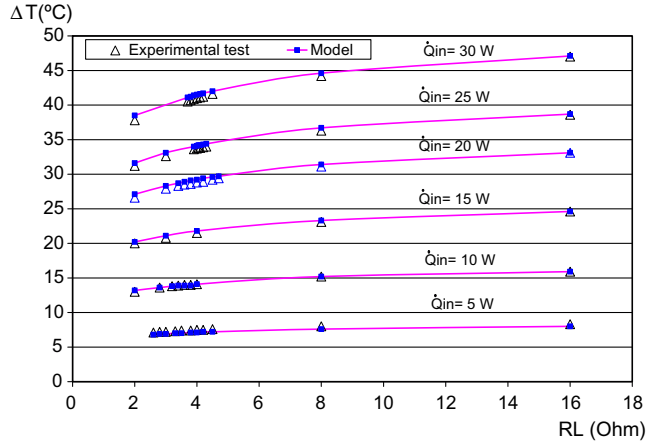

Fig. 6. Temperatura gap between the faces of the Peltier module as a function of the load resistance R_L for a constant supplied heat flux.

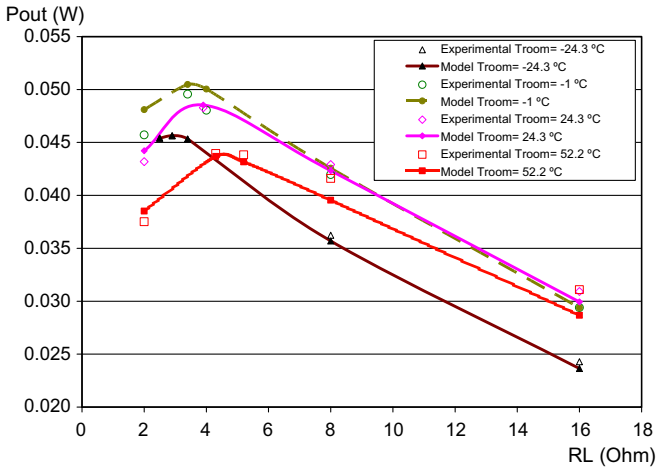

Fig. 7. Thermoelectric generated power for a room temperature constant with a supplied heat flux of 9.97 W.

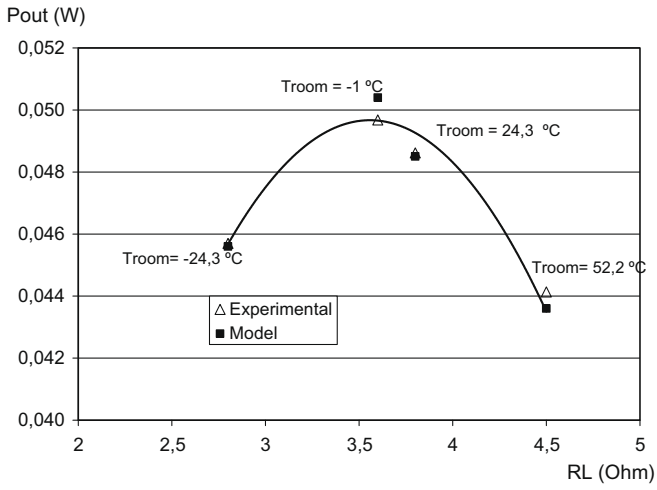

Fig. 8. Maximum power for each curve of constant room temperature, with a supplied heat flux of 9.97 W.

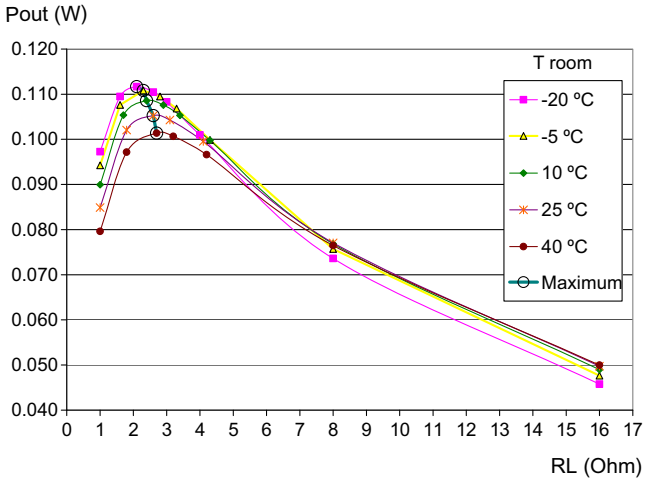

Fig. 9. Thermoelectric generated power for a constant room temperature, with a temperature gap between the faces of the module of 20 °C.

If we suppose that the thermoelectric properties do not depend on the temperature, for the tests where the heat flux was constant, the value of the electric power generated would be constant, independent of the room temperature. Experimentally, we have checked that this supposition is not correct, see Fig. 7.

The model and experimental values are shown in Fig. 7, where it can be checked that the errors are lower than 5%.

Fig. 8 shows the maximum power curve (for a constant room temperature, Fig. 7). The maximum of the power curve is produced for a load resistance that is greater as the room temperature is greater. For this case of study, the curve of maximum power has a parabolic shape, reaching the highest value for a room temperature of −1 °C. The influence of the temperature on the thermoelectric properties depends on the material used, so with other Peltier modules, different curves would be obtained.

5.3. Case III: Constant temperature gap between the faces of the Peltier module varying the room temperature and the electric load resistance

5.3.1. Output thermoelectric power experimental and simulated

In order to check the influence of the room temperature, the cases where the temperature gap between the faces of the Peltier module is constant have been simulated. The electric power generated is shown in Fig. 9, for a constant temperature gap of 20 °C, with varying the load resistance.

If we suppose that the thermoelectric properties are not a function of the temperature, for the tests where the temperature gap of the faces of the Peltier module is constant, the maximum power generated (calculated using the model of an ideal thermocouple or the models that suppose average values for the thermoelectric properties) would be constant, independent of the room temperature. However, the simulations and the experimental data show that this is not correct.

For the case of our study, Fig. 9, a decrease of 9% of the maximum power generated was obtained between the lowest room temperature, $T_{room} = -20$ °C, and the highest, $T_{room} = 40$ °C, for a constant temperature gap between the faces of the Peltier module of 20 °C.

For lower values of load resistance, the generated power is greater as the room temperature is lower. For higher values of room temperature, the generated power is greater as the room temperature is greater, as shown in Fig. 9.

Our simulations allow choosing the load resistance more suitably as a function of the ambient (room) temperature of operation.

6. Conclusions

- A complete computational model has been developed that is capable to simulate the thermoelectric generation of the Peltier module. It solves the equations of thermoelectricity and the heat transfer phenomenon. The thermoelectric parameters are defined as functions of temperature, which allows us to keep in mind the Thomson effect.
- The computational model has been validated using experimental data of a test bench for different room temperatures and different heat fluxes. The errors are lower than 5%.
- Our computational model has important advantages relative to other calculation methods from the literature such as:
  - The model determines the thermoelectric power generated for any boundary conditions of operation (supplied heat flux to the Peltier module and room temperature). It is not necessary to obtain parameters experimentally.
  - It solves the system of equations determining the temperatures of all the elements in the thermoelectric system and the heat fluxes involved. It determines the transitory state as well as the steady state. This makes the model very useful as a design tool of thermoelectric generation systems.
  - The influences of room temperature, residual heat flux and electric load resistance on the behavior of the thermoelectric generation system were studied.
  - It was experimentally proved and demonstrated that the electric load resistance that gives the maximum power varies with the supplied heat flux. Specifically, in our case of study, it raises 18% when the electric load value is increased from 3.3 Ω (5 W) to 3.9 Ω (30 W). This effect can be observed in the computational model as well.
  - For a constant supplied heat flux, it has been verified that the maximum power obtained is a function of the room temperature and the load resistance. For the case of a supplied heat flux of 9.97 W, the curve of the maximum power as a function of the room temperature has a parabolic shape, reaching the maximum at the temperature of −1 °C.
  - For a constant temperature gap between the faces of the Peltier module, the influence of the room temperature on the maximum power was studied. In our case, a decrease of 9% of the maximum power generated was obtained between the lowest simulated room temperature, −20 °C, and the highest room temperature, 40 °C.

References

[1] Benson DK, Jayadev TS. Thermoelectric energy conversion-economical electric power from low grade heat. Proceedings of the third international conference on thermoelectric energy conversion Arlington, TX, vol. 12–14. New York: IEEE; 1980. p. 27–56.
[2] Rowe DM. CRC Handbook of thermoelectrics; 1995. p. 19–25. ISBN 0-83-0146-7.
[3] Ioffe AF. Semiconductor thermoelements and thermoelectric cooling. London: Infosearch Ltd; 1957.
[4] Goldsmid HJ. Conversion efficiency and figure-of-merit. In: Rowe DM, editor. CRC handbook of thermoelectrics. New York (USA): CRC Press; 1995. p. 19–25.
[5] Nolas GS, Sharp J, Goldsmid HJ. Historical development. In: New materials developments. Australia: Springer; 2001. p. 1–13.
[6] Rowe DM, Min G. Evaluation of thermoelectric modules for power generation. J Power Sources 1998;73:193–8.
[7] Rowe DM, Min G. Design theory of thermoelectric modules for electrical power generation. IEE Proc Sci Meas Technol 1996;143(6):351–6. ISSN 1350-2344.
[8] Omer SA, Infield DG. Design optimization of thermoelectrics devices for solar power generation. Sol Energy Mater Sol Cells 1998;53:67–82.
[9] Rowe DM, Min G. Optimisation of thermoelectric module geometry for 'waste heat' electric power generation. J Power Sources 1992;38:253–9.
[10] Wu C. Analysis of waste-heat thermoelectric power generators. Appl Therm Eng 1996;16:63–9.

[11] Nuwayhid R et al. On entropy generation in thermoelectric devices. Energy Convers Manage 2000;41:891–914.
[12] Arenas A. Thesis Doctoral: ''Determinación de nuevos criterios que permitan la optimización de parámetros de diseño de una bomba de calor por efecto Peltier", Departamento de Fluidos y Calor. Universidad Pontificia Comillas, Madrid; 1999.
[13] Yu G, Chen L. Theoretical revision on DT-I formula for A.F. Ioeffés thermoelectric cooling. In: Proceedings of the 11th International conference on thermoelectrics, Arlington, Texas, USA; 1992. p. 282–4.
[14] Lau PG, Buist RJ. Temperature and time dependant finite-element model of a thermoelectric couple. In: Proceedings of the 15th International conference on thermoelectrics; 1996. p. 227–33.
[15] Lau PG, Buist RJ. Calculation of thermoelectric power generation performance using finite element analysis. In: Proceedings of the 16th International conference on thermoelctrics; 1997. p. 563–66.
[16] Stockholm JG, Stockholm DW. Thermoelectric modelling of a cooling module with heat exchangers. In: Proceedings of the 12th International conference on thermoelctrics; 1992. p. 140–6.
[17] KondratievD, Yershova L. TE coolers computer simulation: incremental upgrading of rate equations approch. In: Proceedings of the 6th European workshop on thermoelectrics, Freiburg, Germany; 2001. p. 204–11.
[18] Astrain D, Vián JG, Albizua J. Computational model for refrigerators based on Peltier effect application. Appl Therm Eng 2005:3149–62.
[19] Vián JG, Astrain D, Aguas JJ. Thermoelectric equipment to keep laboratory test-tube at a controlled temperature. J Thermoelectr 1999;3:52–65.
[20] Vián JG, Astrain D, Dominguez M. Numerical modelling and design of a thermoelectric dehumidifier. Appl Therm Eng 2002:407–22.
[21] Ritzer TM, Lau PG. Economic optimization of heat sink design. In: Proceedings of the13th international conference on thermoelectrics, Kansas City, MO; 1994. p. 77–100.